ST2L expression on monocyte subsets is associated with acute coronary syndrome severity and plaque vulnerability

Peinan Ju, Jianhui Zhuang*, Shekhar Singh, Yuyan Lyu, Xiankai Li*

Department of Cardiology, Shanghai Tenth People's Hospital, Tongji University School of Medicine, Shanghai, China

Submitted: 12 March 2020; **Accepted:** 2 September 2020
Online publication: 3 May 2021

Arch Med Sci 2026; 22 (4): 2295–2306
DOI: https://doi.org/10.5114/aoms/127176

***Corresponding authors:**
Jianhui Zhuang MD, PhD
Xiankai Li, MD, PhD
Department of Cardiology
Shanghai Tenth
People's Hospital
Tongji University
School of Medicine
301 Middle Yanchang Road
Shanghai 200072,
China
E-mail: jh_zhuang@tongji.edu.cn;
lixiankai@tongji.edu.cn

Abstract

Introduction: Pro-inflammatory monocyte infiltration and conversion to macrophages are established contributors to acute coronary syndrome (ACS) and plaque instability as visualized by optical coherence tomography (OCT). Increased serum levels of soluble ST2 isoform (sST2) predict poor outcomes in patients with ACS and heart failure. However, whether the transmembrane ST2 isoform (ST2L) can be used to assess the severity of ACS and plaque vulnerability early in the disease course remains elusive.
Material and methods: Flow cytometry and ELISA were performed to evaluate the levels of ST2L on different monocyte subsets in ACS patients and serum concentration of sST2. Bone marrow-derived macrophages were isolated and then polarized to M1 or M2 phenotype, and ST2L expression levels were detected by quantitative RT-PCR and immunoblotting.
Results: We observed that the proportion and absolute number of ST2L expressing cells among monocyte subsets 1 (Mon1) and Mon2 were significantly lower, accompanied with increased serum sST2, in ACS patients as compared to controls. However, only the proportion of $ST2L^+$/Mon2 was closely associated with the severity of atherosclerotic plaques. With regard to plaque instability, patients with thin cap fibrous atheroma (TCFA) identified by optical coherence tomography (OCT) had a lower absolute number (non-TCFA $1.26 \times 10^4 \pm 0.63 \times 10^4$/ml vs. TCFA $0.92 \times 10^4 \pm 0.37 \times 10^4$/ml, $p = 0.034$) and lower percentage (non-TCFA 17.65% ±3.10% vs. TCFA 13.17% ±2.29%, $p < 0.001$) of $ST2L^+$/Mon2 than those without TCFA. In multivariate analysis, the proportion of $ST2L^+$/Mon2 was independently associated with TCFA. In bone marrow-derived macrophages, sST2 and ST2L were highly expressed in M2 macrophage.
Conclusions: Compared to circulating sST2, the proportion of ST2L-expressing Mon2 subsets was more strongly associated with the severity of ACS and plaque vulnerability.

Key words: acute coronary syndrome, macrophage polarization, monocyte subset, plaque progression, ST2.

Introduction

Acute coronary syndrome (ACS) is reported to be one of the most important causes of mortality and morbidity worldwide [1]. It is widely accepted that plaque rupture or erosion followed by obstructive thrombus formation is the main feature of ACS. Based on quantitative analysis of

coronary angiography, it is evident that diverse parameters, including the presence of coronary plaque and the degree of luminal stenosis, carry incremental predictive value and improve risk stratification of ACS [2]. On the other hand, intravascular optical coherence tomography (OCT) is considered to generate high-resolution cross-sectional images of plaque morphology, allowing physicians to visualize the development of the distinct vulnerable plaques characterized by a rupture-prone thin fibrous cap and a lipid-rich necrotic core [3]. In addition, thin cap fibrous atheroma (TCFA) is more likely to have higher numbers of pro-inflammatory macrophages, with punctate signal-rich spots exceeding the background noise on OCT images [4].

Suppression of tumorigenicity 2 (ST2), a member of the interleukin 1 receptor (IL-1R) family, constitutes two primary isoforms regulated by IL-33 [5, 6]. The transmembrane ST2 receptor (ST2L) consists of a membrane-bound isoform with 3 extracellular IgG domains, while a soluble ST2 receptor (sST2), lacking transmembrane and intracellular domains, acts as an IL-33 decoy receptor and could be detected in circulating serum [7]. Growing evidence has expanded our knowledge about the biology function of IL-33/ST2 signaling and the pathogenesis of IL-33/ST2 in tumor development and cardiovascular abnormality [8, 9]. Depletion of ST2 in a mouse pressure overload model results in excessive ventricular hypertrophy, chamber dilation, and cardiac fibrosis [10]. Moreover, increased serum sST2 predicts poor outcomes in patients with ACS and chronic heart failure [6, 11–14]. By contrast, ST2L, predominantly expressed in macrophages, activates Th2 cells and mast cells, retards atherosclerotic development and alleviates cardiac remodeling through interaction of IL-33 and enhancement of its intracellular signaling [15]. However, the association of ST2L, especially ST2L expression on monocyte subsets, with plaque characteristics remains unknown. Therefore, we aimed to determine the association of sST2 and ST2L expression on monocyte subsets with the severity and vulnerability of coronary plaques in this study.

Material and methods

The data that support the findings of this study are available from the corresponding author upon reasonable request.

Study population

Forty-eight patients with unstable angina pectoris (UAP) and 31 patients with ST-elevation myocardial infarction (STEMI) admitted to Shanghai Tenth People's Hospital between April 2013 and July 2014 were recruited as previously described [16]. UAP was diagnosed based on the manifestation of angina at rest, accelerated chest pain, or new-onset chest pain without any abnormality of cardiac markers. STEMI was diagnosed according to the criteria of the Fourth Universal Definition of Myocardial Infarction [17] and further confirmed by coronary angiography, with the presence of acute thrombosis secondary to plaque rupture. Thirty-three age- and sex-matched subjects with suspected angina but free of luminal diameter narrowing ≥ 50% confirmed by angiography served as controls. Patients with severe liver and kidney failure, acute infectious disease, and malignancies were excluded. All patients provided written informed consent before enrollment. The study was approved by Shanghai Tenth People's Hospital and followed the guidelines of the Declaration of Helsinki.

Quantification of plaque characteristics by angiography and optical coherence tomography

Coronary angiography and optical coherence tomography (OCT) were performed as previously described [16]. We defined the severity of ACS by evaluating the severity of coronary plaques obtained from coronary angiography. The severity of coronary plaques was evaluated by the length of plaque (> 20 mm as long lesions), the degree of stenosis (moderate [from 50% to 69%]; severe [from 70% to 99%], or occlusion [100%]) with or without calcification, and the number of coronary vessels with significant stenosis. Left main trunk stenosis was considered as a two-vessel disease. TCFA was defined as a plaque presenting lipid content for > 90°, and with thinnest part of the fibrous cap measuring < 65 µm obtained from OCT [17, 18].

Analysis of serum sST2

Approximately 5 ml of peripheral venous blood was collected from controls and UAP patients on the day after fasting for over 8 h. Peripheral venous blood from patients with STEMI was collected and placed in EDTA-coated tubes on the day of admission. After centrifugation, serum was stored at –80°C for further analysis in batches. Serum levels of sST2 were measured by sandwich enzyme immunoassay using Human ST2/IL-33R Quantikine ELISA kits (catalog #DST200, R&D System, USA) according to the manufacturer's protocol. The coefficients of variation (CV) for intra-assay precision and inter-assay precision were less than 5.2% and 6.8%, respectively.

Quantification of ST2L on monocyte subsets by flow cytometry

For measurement of surface ST2L expression on monocytes, 100 µl of peripheral blood was

blocked with 1% bovine serum albumin (BSA, Gibco, USA) solution for 15 min at 4°C and stained with a cocktail of monocyte antibodies for 30 min at 4°C. The information and concentrations of each monocyte subset are shown in Supplementary Table SI. On the basis of flow cytometry, circulating monocytes were divided into $CD14^{++}CD16^{-}$ monocytes (Mon1), $CD14^{++}CD16^{+}$ monocytes (Mon2), and $CD14^{+}CD16^{+}$ monocytes (Mon3). PerCP-eFluor710-conjugated antibodies against IL-33R(ST2) were used to analyze the expression of ST2 receptors on monocytes (Figure 1). The flow cytometry for identifying surface ST2L expression and monocyte subsets was performed by one expert technician who was blinded to the coronary angiography and OCT results [16].

Induction of macrophage polarization

Animal studies were conducted in accordance with the Guide for the Care and Use of Laboratory Animals (U.S. National Institutes, MD, USA), and all the procedures were approved by the Animal Care and Use Committee of Shanghai Tenth People's Hospital. Bone marrow cells were isolated from femurs of C57BL/6 mice following standard protocol in Dulbecco's modified Eagle's medium (DMEM, Gibco, USA) containing 10% fetal bovine serum (FBS, Gibco, USA) and 1% penicillin and streptomycin [19]. Following separation, bone marrow-derived macrophages (BMDMs) were cultured in 10% FBS/DMEM with recombinant M-CSF at a concentration of 100 ng/ml (Peprotech Incorporation, USA) for 3 days (M0 phenotype). BMDMs were washed and treated for 12 h with DMEM + 5% FBS alone, LPS at a concentration of 100 ng/ml, and recombinant interferon gamma (IFN-γ, Peprotech Incorporation, USA) at a concentration of 20 ng/ml for polarization to the M1 phenotype, or recombinant IL-4 at a concentration of 20 ng/ml (Peprotech Incorporation, USA) for polarization to the M2 phenotype. Likewise, human circulating monocytes were collected from healthy volunteers, differentiated into macrophages and maintained RPMI 1640 medium (Gibco, USA) supplemented with 10% FBS according to previous protocols [20].

Quantitative RT-PCR

Total cellular RNA was extracted and purified using TRIzol reagent (Invitrogen, USA). Reverse transcription was performed using the Transcriptor First Strand cDNA Synthesis Kit (Roche, Germany). Quantitative RT-PCR for ST2L, TNF-α, IL-6, CD206, and Arg-1 was performed using FastStart Universal SYBR Green Master Mix (Roche, Germany) on a Roche LightCycler instrument. The primer sequences used for quantitative RT-PCR are tabulated in Supplementary Table SII.

Immunoblotting

Protein lysates were performed on 8% SDS-PAGE gels and transferred to membranes as our previ-

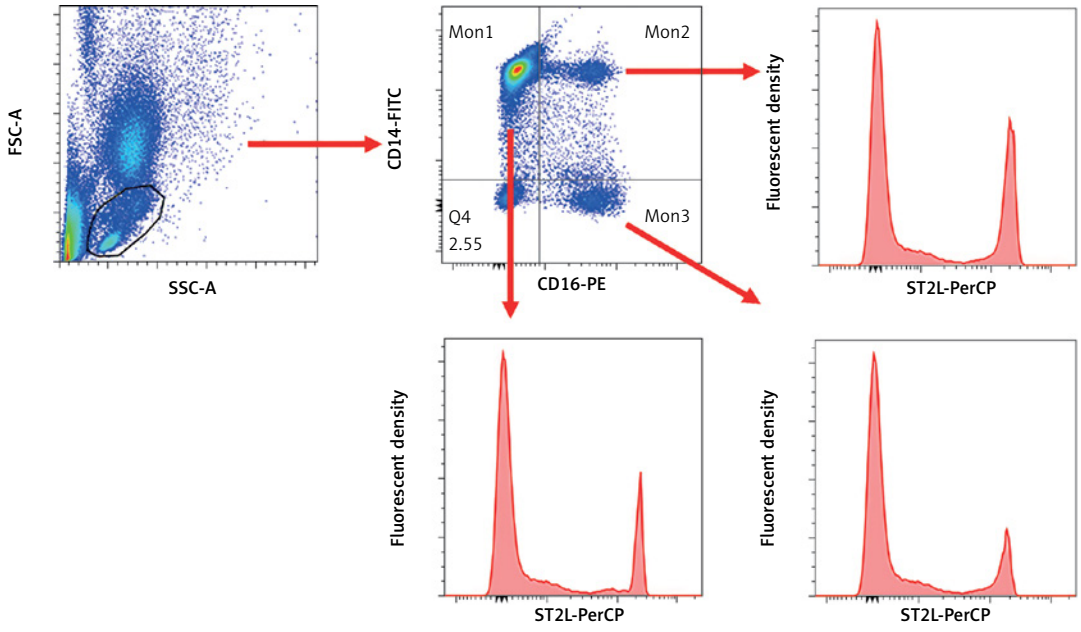

Figure 1. Gating strategy for circulating monocyte subsets and ST2L expression. Whole peripheral blood cells were prepared and labeled with various antibodies. CD14 was used in conjunction with CD16 to identify monocyte subsets (Mon). Mon1 was identified as $CD14^{++}CD16^{-}$, Mon2 as $CD14^{++}CD16^{+}$, and Mon3 as $CD14^{+}CD16^{+}$. ST2L antibodies were further used to stratify the percentage of ST2L positive monocyte subsets

ously reported [21]. The membranes were probed using antibody directed against ST2L (Abcam, USA) and normalized to GAPDH (Santa Cruz, USA).

Statistical analysis

Continuous variables were presented as mean ± standard deviation (SD). Categorical variables were presented as absolute number and proportion. Differences between two groups were analyzed with Student's *t* test. Differences between multiple groups were initially compared using one-way ANOVA, and post-hoc tests were then performed with Bonferroni correction. Receiver-operating characteristic (ROC) curve analysis was conducted to determine the performance of serum sST2 and ST2L expression on monocytes for assessing plaque vulnerability. Youden's index was applied to derive the best cut-off value of ST2L expression on monocytes. Based on the cut-off, we then performed backward stepwise multivariate logistic regression that included variables with $p < 0.1$ in univariate analysis to identify independent predictors of plaque vulnerability. Values of $p < 0.05$ were considered significant.

Results

Comparison of serum sST2 and ST2L on monocytes among patients with different severity of ACS

The patient characteristics, angiographic findings, and results of OCT imaging were summarized in our previous study [16]. Of the whole measurements, the proportions and the absolute number of ST2L on monocytes and Mon2 subsets in STEMI patients were significantly lower than those in UAP patients and controls (Table I). Consistent with other research, serum levels of sST2 showed a steady increase from controls to STEMI patients (control 1.35 ±0.65 ng/ml, UAP 2.42 ±0.61 ng/ml and STEMI 3.88 ±1.61 ng/ml, $p < 0.001$).

Based on quantitative analysis of coronary angiography, it is evident that diverse parameters, including the presence of coronary plaque and the degree of luminal stenosis, carry incremental predictive value and improve risk stratification of ACS [2]. We next assessed the association of serum sST2 and ST2L expression on monocyte subsets with the severity of ACS as detected by angiography. No significant association was found between serum sST2 and the atherosclerotic severity of ACS (Figures 2 A, E, I). ACS patients with lower proportions of $ST2L^+$/Mon and $ST2L^+$/Mon1 were more likely than those with higher proportions to have obstructive stenosis (Figures 2 B, F, J). It should be noted that the percentage of $ST2L^+$/Mon2 was significantly inversely correlated with all three angiographic parameters (Figures 2 D, H, L).

Relation of serum sST2 and ST2L expression on monocyte subsets to plaque stability

Plaque characteristics determined by OCT were summarized in our previous study. Of the OCT subgroup, patients with TCFA had a lower absolute number (non-TCFA $1.26 \times 10^4 \pm 0.63 \times 10^4$/ml vs. TCFA $0.92 \times 10^4 \pm 0.37 \times 10^4$/ml, $p = 0.034$) and lower percentage (non-TCFA 17.65% ±3.10% vs. TCFA 13.17% ±2.29%, $p < 0.001$) of $ST2L^+$/Mon2 than those without TCFA (Table II). However, there was no difference in serum levels of sST2 between groups (Table II). We then analyzed the association of serum sST2 and ST2L expression on monocytes with plaque morphology, and found that serum sST2 was positively correlated with fibrous cap thickness (Pearson $r = 0.306$, $p = 0.034$), while no differences in serum sST2 levels according to lipid

Table I. Comparison of serum sST2 levels and ST2L expression on monocytes among the three groups

Parameter	Control (n = 33)	UAP (n = 48)	STEMI (n = 31)	*P*-value	*P* (group 1 vs. 2)	*P* (group 2 vs. 3)
sST2 [ng/ml]	1.35 ±0.65	2.42 ±0.61	3.88 ±1.61	< 0.001	< 0.001	< 0.001
$ST2L^+$Mon (%)	21.7 ±3.76	14.9 ±1.83	9.34 ±2.48	< 0.001	< 0.001	< 0.001
$ST2L^+$Mon1 (%)	25.0 ±3.93	16.8 ±2.39	9.84 ±3.02	< 0.001	< 0.001	< 0.001
$ST2L^+$Mon2 (%)	20.9 ±2.29	15.8 ±3.56	10.13 ±1.52	< 0.001	< 0.001	< 0.001
$ST2L^+$Mon3 (%)	5.13 ±1.30	4.36 ±1.38	4.89 ±1.24	0.029	0.033	0.249
$ST2L^+$Mon, 10^4/ml	9.17 ±4.28	6.62 ±2.52	6.41 ±2.64	0.001	0.002	1.000
$ST2L^+$Mon1, 10^4/ml	7.58 ±3.78	5.23 ±2.08	4.94 ±2.21	< 0.001	0.001	0.003
$ST2L^+$Mon2, 10^4/ml	1.30 ±0.63	1.12 ±0.56	1.16 ±0.49	0.370		
$ST2L^+$Mon3, 10^3/ml	2.88 ±1.87	2.68 ±1.85	3.11 ±1.61	0.584		

Data are presented as mean ± SD. P (group 1 vs. 2) indicates the difference between Control and UAP groups after post-hoc Bonferroni comparison. P (group 2 vs. 3) indicates the difference between UAP and STEMI groups after post-hoc Bonferroni comparison. UAP – unstable angina pectoris, STEMI – ST-elevation myocardial infarction, ST2 – suppression of tumorigenicity 2, ST2L – transmembrane ST2 isoform, Mon – monocytes.

core arc and minimum lumen area were observed (Table III). In contrast, the percentage of ST2L$^+$/Mon2 gradually increased with increasing fibrous cap thickness (Pearson $r = 0.523$, $p < 0.001$), whilst there was an inverse correlation between percentage of ST2L$^+$/Mon2 and lipid core arc (Pearson $r = -0.473$, $p = 0.001$).

ST2L on Mon2 as determinants of plaque vulnerability

The area under the ROC curve of percentage and absolute number of ST2L$^+$/Mon2 for determining TCFA was 0.889 and 0.663, respectively (Figure 3). The optical percentage of ST2L$^+$/Mon2 cutoff to

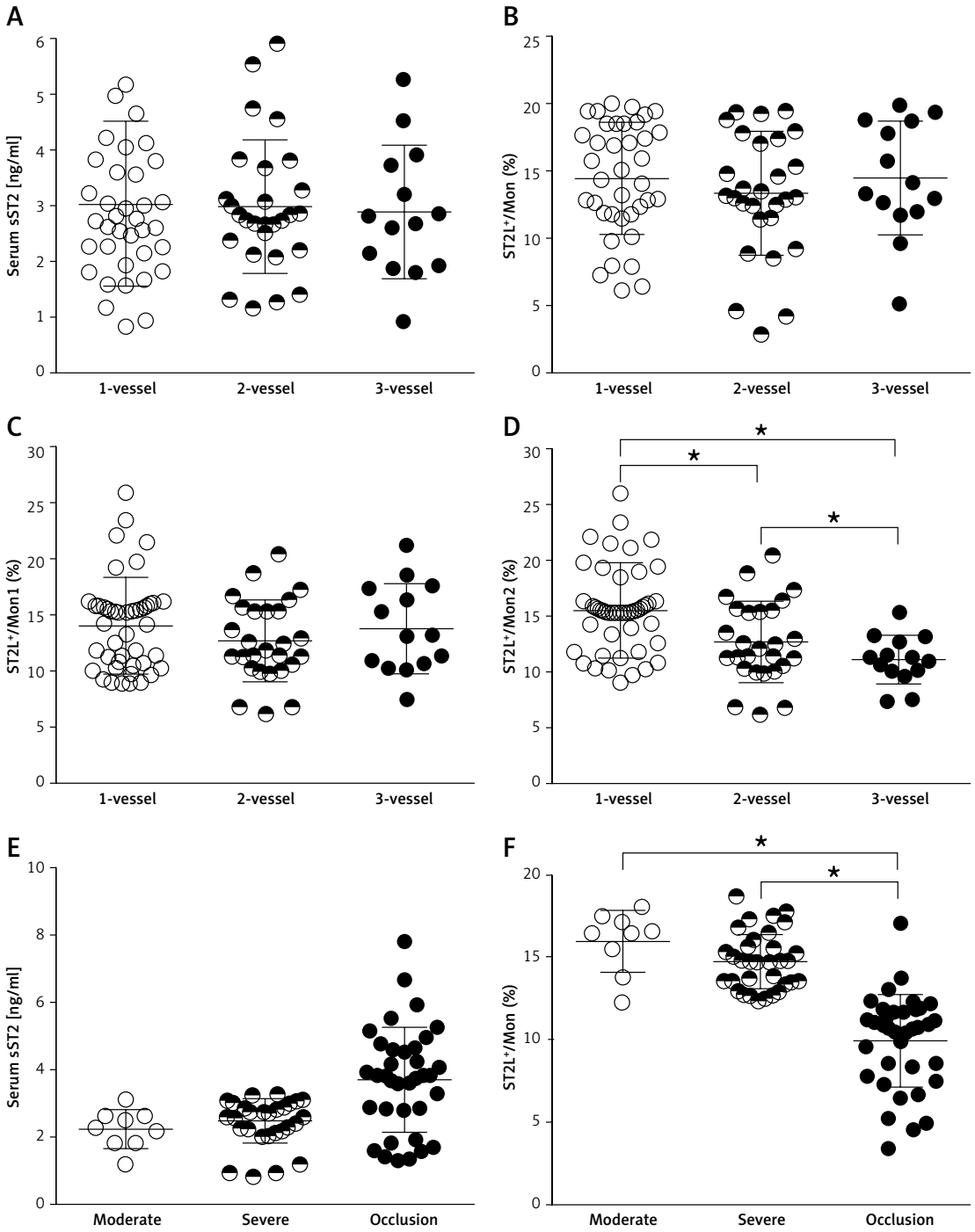

Figure 2. Comparison of serum sST2 and the percentage of ST2L expression on monocytes in patients with different severities of coronary plaques detected by angiography. **A**–**D** – Comparison of serum sST2 and the percentage of ST2L expression on monocytes according to the number of stenotic vessels. **E**–**F** – Comparison of serum ST2 and the percentage of ST2L expression on monocytes according to the degree of stenosis

*ST2 = suppression of tumorigenicity 2, ST2L = transmembrane ST2 isoform, Mon = monocyte. *P < 0.05.*

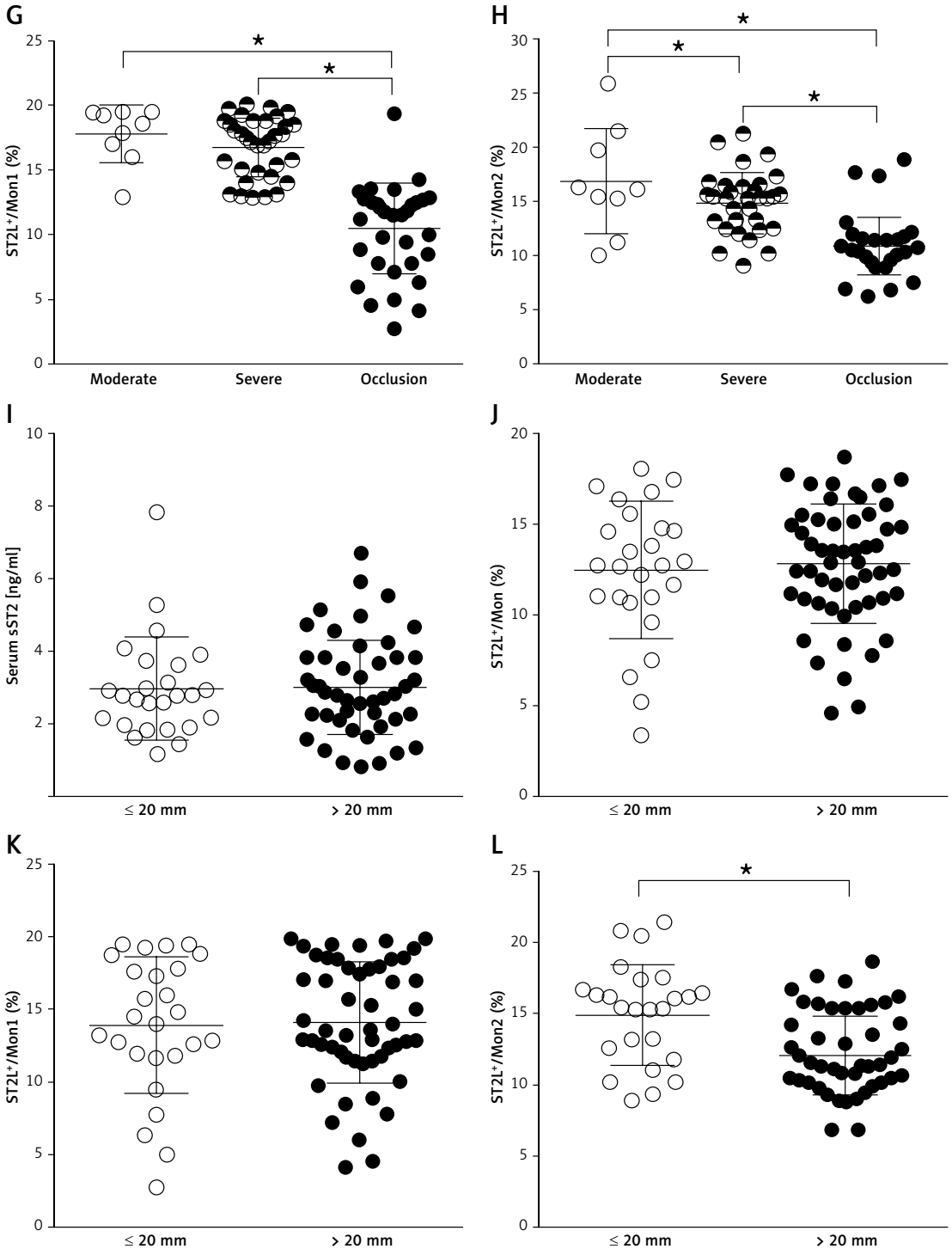

Figure 2. Cont. **G–H** – Comparison of serum ST2 and the percentage of ST2L expression on monocytes according to the degree of stenosis. **I–L** – Comparison of serum ST2 and the percentage of ST2L expression on monocytes according to the lesion length

*ST2 = suppression of tumorigenicity 2, ST2L = transmembrane ST2 isoform, Mon = monocyte. *P < 0.05.*

predict TCFA was 15.31%, which showed sensitivity of 82.41 and specificity of 85.71 (Figure 3).

After correction for known clinical risk factors including age, sex, smoking, hypertension, diabetes mellitus, white blood cells (WBC), low-density lipoprotein cholesterol (LDL-C), and the percentage of circulating Mon2 subsets, decreased levels of percentage of ST2L$^+$/Mon2 remained an independent predictor of TCFA (OR = 0.07, 95% CI: 0.02–0.29, $p < 0.001$, Table IV).

Table II. Comparison of serum sST2 and ST2L expression on monocytes in patients with and without TCFA

Parameter	Non-TCFA (n = 28)	TCFA (n = 20)	P-value
sST2 [ng/ml]	2.54 ±0.53	2.24 ±0.69	0.096
ST2L$^+$Mon (%)	14.74 ±1.90	15.03 ±1.77	0.595
ST2L$^+$Mon1 (%)	16.29 ±2.45	17.41 ±2.21	0.110
ST2L$^+$Mon2 (%)	17.65 ±3.10	13.17 ±2.29	< 0.001
ST2L$^+$Mon3 (%)	4.51 ±1.52	4.14 ±1.14	0.361
ST2L$^+$Mon, 10^4/ml	7.18 ±2.77	5.84 ±1.93	0.069
ST2L$^+$Mon1, 10^4/ml	5.59 ±2.29	4.72 ±1.68	0.153
ST2L$^+$Mon2, 10^4/ml	1.26 ±0.63	0.92 ±0.37	0.039
ST2L$^+$Mon3, 10^3/ml	3.20 ±2.08	1.96 ±1.18	0.021

Data are presented as mean ± SD. TCFA – thin cap fibrous atheroma. Other abbreviations listed as in Table I.

Table III. Correlation of serum sST2 levels and ST2L expression on monocytes with plaque morphology

Parameter	Fibrous cap thickness		Arc of lipid core		MLA	
	r	P-value	r	P-value	r	P-value
sST2 [ng/ml]	0.306	0.034	0.076	0.608	0.257	0.078
ST2L$^+$Mon (%)	–0.239	0.101	–0.099	0.505	0.078	0.599
ST2L$^+$Mon1 (%)	–0.245	0.094	–0.245	0.094	–0.123	0.405
ST2L$^+$Mon2 (%)	0.523	< 0.001	–0.473	0.001	0.265	0.069
ST2L$^+$Mon3 (%)	0.203	0.167	0.292	0.044	0.146	0.321
ST2L$^+$Mon, 10^4/ml	–0.010	0.947	0.165	0.262	0.054	0.714
ST2L$^+$Mon1, 10^4/ml	–0.101	0.494	0.114	0.440	0.065	0.662
ST2L$^+$Mon2, 10^4/ml	0.264	0.070	–0.215	0.142	0.047	0.750
ST2L$^+$Mon3, 10^3/ml	0.203	0.166	0.310	0.032	–0.133	0.369

MLA – minimum lumen area. Other abbreviations listed as in Table I.

ST2L was primarily expressed in M2 macrophages

It is well known that with the development of atherosclerosis, BM-derived circulating monocytes possess the capacity to differentiate into two macrophage subsets based on their pathologic function and expressions of divergent cytokines [22]. To examine the abundance of ST2L on the macrophage subsets, we induced BMDMs and human macrophages by different stimuli, and confirmed the results by quantitative PCR and immunoblots (Figure 4 A). As compared to M1 macrophages, both ST2L mRNA and protein expression levels were higher in M2 polarized macrophages, suggesting the potential involvement of ST2L in regulating plaque instability (Figures 4 B–D). Interestingly, we found that the concentration of sST2 in the supernatant of M2 macrophages was higher than that of M1 macrophages differentiated from human circulating monocytes (Figure 4 E).

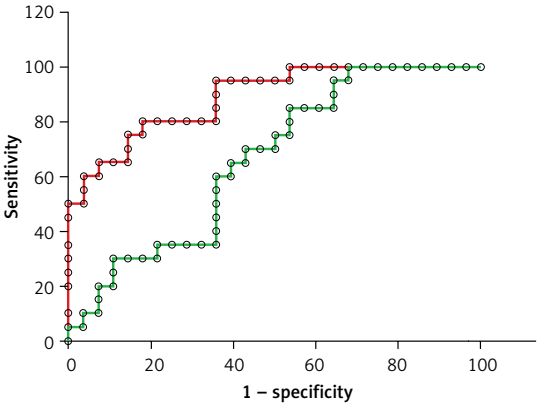

	AUC	P-value
ST2L$^+$/Mon2 (10^4/ml)	0.663	0.057
ST2L$^+$/Mon2 (%)	0.889	< 0.001

Figure 3. Receiver-operating characteristics (ROC) curve analysis showing the discriminative ability of the absolute number and percentage of ST2L$^+$/Mon2 for thin cap fibrous atheroma (TCFA)

AUC – area under the curve.

Discussion

To the best of our knowledge, we demonstrated for the first time that ST2L expression on Mon2, particularly the percentage of ST2L$^+$/Mon2 among circulating leukocytes, was closely associated with the incidence and severity of ACS. The percentage of ST2L$^+$/Mon2, rather than serum sST2, appeared to be a more suitable biomarker

Table IV. Multivariate logistic regression analysis for predictors of TCFA

Parameter	Univariate analysis		Multivariate analysis	
	OR (95% CI)	*P*-value	OR (95% CI)	*P*-value
Age (≥ 65 years)	1.07 (0.30–3.78)	0.92		
Sex	3.57 (0.77–16.54)	0.10		
Smoking	2.05 (0.61–6.82)	0.24		
Hypertension	0.64 (0.17–2.37)	0.50		
Diabetes mellitus	2.57 (0.62–10.71)	0.19		
WBC [10^9/l]	0.97 (0.70–1.34)	0.85		
LDL-C [mg/dl]	0.92 (0.43–1.98)	0.83		
sST2 (> 2.51 ng/ml)	0.39 (0.12–1.27)	0.12		
Mon2 (> 10.6 %)	4.20 (1.23–14.37)	0.02	1.16 (0.28, 4.79)	0.84
$ST2^+$/Mon2 (> 15.31 %)	0.07 (0.02–0.29)	< 0.001	0.07 (0.02, 0.29)	< 0.001
$ST2^+$/Mon2 (> 0.012 × 10^4/ml)	0.37 (0.11–1.25)	0.11		

WBC, LDL-C, HDL-C were defined as continuous variables. P-values were calculated by Wald type test. WBC – white blood cells, HDL-C – high-density lipoprotein cholesterol, LDL-C – low-density lipoprotein cholesterol, OR – odds ratio, other abbreviations listed as in Table I.

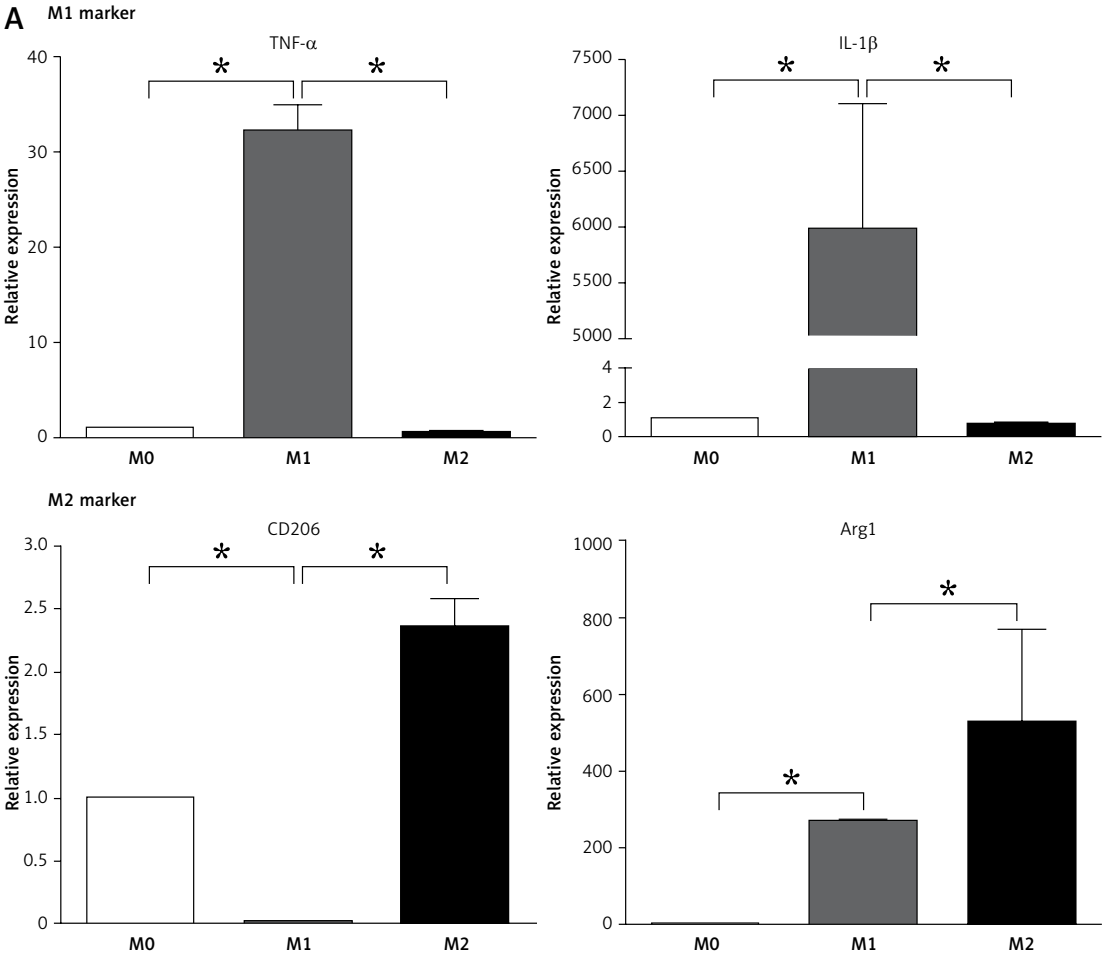

Figure 4. ST2L accumulates in M2 macrophages. **A** – Quantification of M1 and M2 markers in BM-derived macrophages. Macrophages were induced by LPS (100 ng/ml) and IFN-γ (20 ng/ml) for M1 polarization or by IL-4 (20 ng/ml) for M2 polarization. *$P < 0.05$

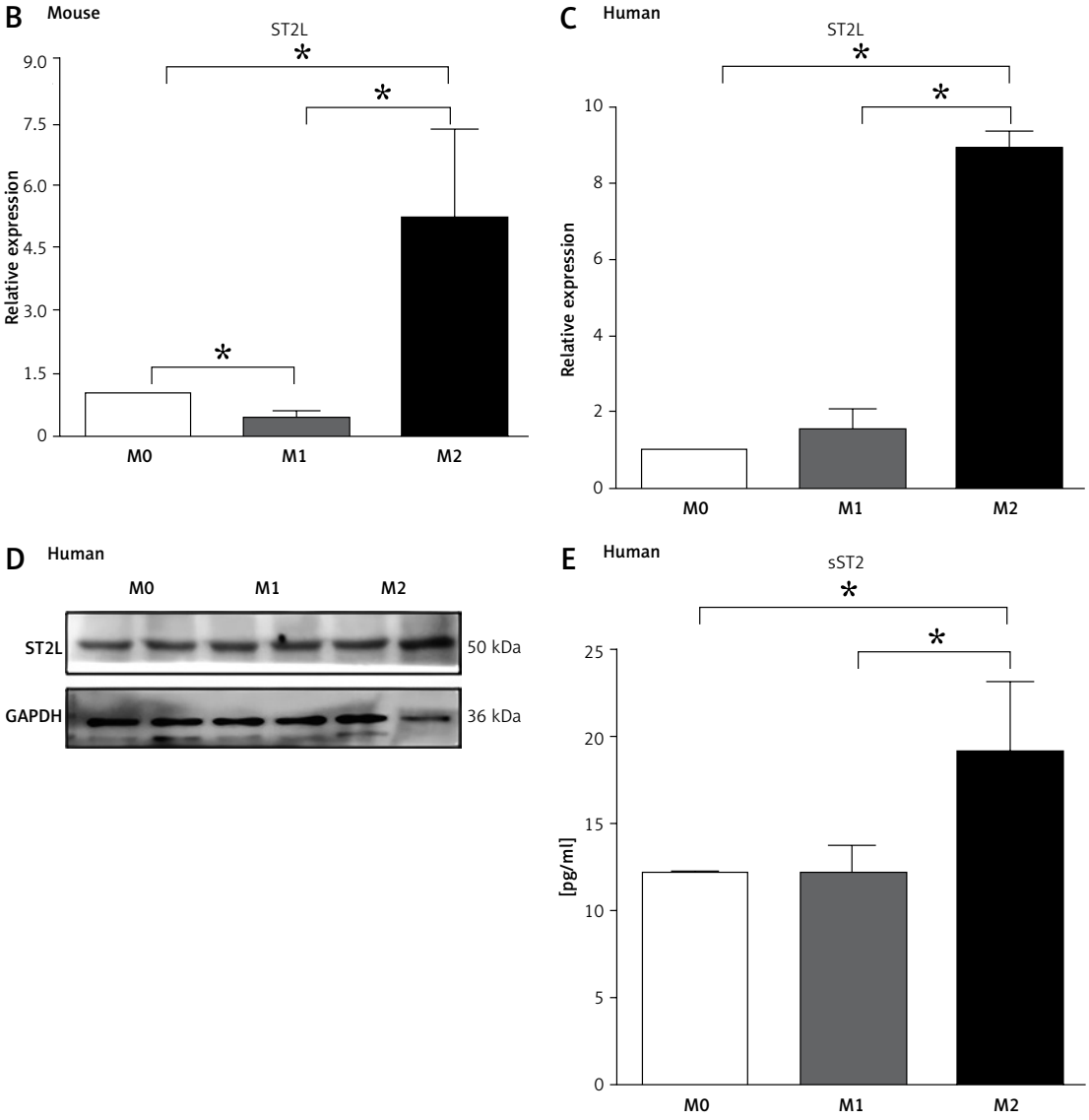

Figure 4. Cont. **B**, **C** – Quantitative PCR indicated that ST2L was upregulated in M2 polarized phenotype of mouse bone marrow-derived macrophages (**B**) and human macrophages (**C**). **D** – Immunoblotting showed the protein expression of ST2L in M0, M1, and M2 macrophages differentiated from human circulating monocytes. **E** – Comparison of the sST2 levels between the supernatant of M1 and M2 macrophages differentiated from human circulating monocytes. *$P < 0.05$

reflecting the signature of plaque destabilization detected by OCT.

It has been reported that IL-33 was predominantly produced by vascular smooth muscle cells and endothelial cells in response to atherogenic stimuli [8]. Likewise, cardiac hypertrophy and mechanical strain substantially induced IL-33 expression, which was predominantly observed in cardiac fibroblasts [10]. Mechanistically, through neutralization of IL-33, sST2 abrogated the cardioprotective effect of IL-33/ST2 signaling in cardiac fibrosis and hypertrophy [11]. While sST2 acted as a circulating isoform and was ubiquitously expressed in various tissues, the transmembrane isoform ST2L was inducible and primarily located in hematopoietic cells, especially Th2 cells, mast cells, monocytes, and macrophages [23]. In the present study, we found that ST2L was highly expressed in M2 macrophages, suggesting that ST2L might be involved in M2 macrophage activation, which contributes to angiogenesis and anti-inflammation. Consistently, a previous research observed that depletion of ST2L disrupts macrophage polarization to M2 phenotype with decreased M2 macrophage markers [15]. In parallel, the supernatant of M2 macrophages had a higher concentration of sST2 than that of M0 and M1 macrophages.

Weinberg *et al.* [6], for the first time, revealed that elevated serum sST2 predicted higher likelihood of 30-day mortality and heart failure in patients with myocardial infarction. Likewise, while the no-reflow phenomenon reflects impaired

myocardial perfusion and poor prognosis [24], including mortality and heart failure, in ACS patients after percutaneous coronary intervention, Somuncu *et al*. [25] identified serum sST2 as an independent predictor of the no-reflow phenomenon in ACS patients. A recent meta-analysis concluded that ACS patients with higher baseline levels of serum sST2 predicted the increased possibility of all-cause mortality and major adverse cardiac events during follow-up [13]. In parallel, our study confirmed that serum sST2 level was higher in ACS patients than in controls. Nevertheless, there was no significant difference in serum sST2 between UAP patients with and without TCFA, suggesting that serum sST2 may not be considered as a predictor of plaque destabilization.

Nonetheless, little is understood about the association of ST2L with the incidence of ACS and plaque vulnerability. Circulating monocytes extravasate through the endothelium and differentiate into two opposite macrophage subsets, initiating atherosclerosis and regulating plaque stabilization [26]. To be more specific, $CD14^{++}CD16^{-}$ Mon1 subsets and $CD14^{++}CD16^{+}$ Mon2 subsets more readily invade the subendothelium and differentiate into active M1 macrophages, which subsequently contribute to necrotic core formation, matrix degradation, and plaque rupture. Others' and our previous studies have shown that $CD14^{++}CD16^{+}$ Mon2 subsets were closely associated with the incidence of ACS [16, 27]. Furthermore, higher proportions of $CD14^{++}CD16^{+}$ Mon2 subsets were more often found in patients with TCFA [16]. Therefore, together with the involvement of ST2L in macrophage polarization, these data prompted us to further investigate whether ST2L on monocyte subsets could be considered as a potential biomarker for ACS and plaque instability. In this regard, we first observed that ST2L was highly expressed in Mon1 and Mon2 subsets and lower in Mon3 subsets, suggesting that ST2L mainly functioned in pro-inflammatory monocytes which subsequently polarized to M1 macrophages and contributed to plaque development and rupture. Our study further provides evidence that a higher percentage of $ST2L^{+}$/Mon2 is associated with ACS. On the other hand, numerous clinical trials have proposed that integrated measurements of plaque composition, location, and extent based on coronary computed tomography angiography or invasive coronary angiography are capable of accurate risk stratification and prognosis for ACS patients [2, 28]. In this regard, only the proportion of $ST2L^{+}$/Mon2 was prevalently lower in patients with high-risk plaque features, indicating that the proportion of $ST2L^{+}$/Mon2 might represent a promising biomarker for risk stratification of ACS.

Given the high image resolution with OCT, it allows physicians to identify high-risk plaques *in vivo*. We found that, in ACS patients, a higher percentage of $ST2L^{+}$/Mon2 indicated a thinner fibrous cap accompanied by a larger extent of lipid core, both of which serve as early features of plaque instability [29]. Combined with ROC curve and multivariate analysis, we further highlighted the superiority of the percentage of $ST2L^{+}$/Mon2 over other clinical factors in predicting vulnerable plaques. Based on the results of our previous study, the circulating Mon2 subset was considered as an independent predictor of the incidence of definite TCFA. It is therefore plausible to assume that ST2L, especially ST2L expression on the Mon2 subset, through its diverse pathogenic roles and clinical significances in atherosclerosis and myocardial infarction, may further improve the prediction of plaque vulnerability.

Finally, we acknowledge some potential limitations in our research. In the current study, we did not investigate the distribution of ST2L on Th2 in ACS patients. It has been demonstrated that accumulation of pro-inflammatory macrophages in infarcted myocardium and phagocytosis of necrotic cardiomyocytes by macrophages are hallmarks of the early phase of myocardial infarction [30]. While Th1 subsets seem more likely to affect the evolution of ACS, the absolute number of circulating Th2 subsets is relatively low, and there is no prominent difference in circulating Th2 subsets between patients with stable angina and ACS [31]. Despite this, a comprehensive assessment of ST2L on Th2 cells may boost the understanding of IL-33/ST2 signaling in atherosclerotic development. Particularly, a larger number of patients in another external validation cohort is required to strengthen our findings. In multivariate logistic regression analysis for predictors of TCFA, several well-known risk factors including diabetes, WBC, and LDL-C did not show significant effects on TCFA, as reported in previous studies [32–34], which may due to the small size of our study. Moreover, accumulating evidence in the functional characterization of macrophages has revealed that the phenotypes are not limited to the M1 and M2 extremes but rather represent a continuous spectrum of phenotypes associated with differential cytokine production and functional characteristics [35]. Given the difficulty in simulating the environment of macrophages in plaques *in vitro*, we adopted the concepts of M1 and M2 in this study, with M1 primarily representing macrophages showing a proinflammatory phenotype and M2 representing macrophages with an anti-inflammatory phenotype.

In conclusion, an enhanced proportion of $ST2L^{+}$/Mon2 was associated with the severity of ACS and plaque vulnerability in coronary arteries. $ST2L^{+}$/Mon2 might represent a promising biomarker for the early diagnosis of vulnerable plaques.

Acknowledgments

We appreciate patients who participated in this study.

Funding

This study is supported by Grants No. 81800424 and No. 81800378 from the National Natural Science Foundation of China, and by the Fundamental Research Funds for the Central Universities (No. 22120180581).

Ethical approval

The study was approved by Ethics Committee of Shanghai Tenth People's Hospital and all individuals provided written informed concept before participation.

Conflict of interest

The authors declare no conflict of interest.

References

1. Ibanez B, James S, Agewall S, et al. 2017 ESC Guidelines for the management of acute myocardial infarction in patients presenting with ST-segment elevation: The Task Force for the management of acute myocardial infarction in patients presenting with ST-segment elevation of the European Society of Cardiology (ESC). Eur Heart J 2018; 39: 119-77.
2. Hadamitzky M, Achenbach S, Al-Mallah M, et al. Optimized prognostic score for coronary computed tomographic angiography: results from the CONFIRM registry (COronary CT Angiography EvaluatioN For Clinical Outcomes: An InteRnational Multicenter Registry). J Am Coll Cardiol 2013; 62: 468-76.
3. Sinclair H, Bourantas C, Bagnall A, Mintz GS, Kunadian V. OCT for the identification of vulnerable plaque in acute coronary syndrome. JACC Cardiovasc Imaging 2015; 8: 198-209.
4. Cassar A, Matsuo Y, Herrmann J, et al. Coronary atherosclerosis with vulnerable plaque and complicated lesions in transplant recipients: new insight into cardiac allograft vasculopathy by optical coherence tomography. Eur Heart J 2013; 34: 2610-7.
5. Schmitz J, Owyang A, Oldham E, et al. IL-33, an interleukin-1-like cytokine that signals via the IL-1 receptor-related protein ST2 and induces T helper type 2-associated cytokines. Immunity 2005; 23: 479-90.
6. Weinberg EO, Shimpo M, De Keulenaer GW, et al. Expression and regulation of ST2, an interleukin-1 receptor family member, in cardiomyocytes and myocardial infarction. Circulation 2002; 106: 2961-6.
7. Liew FY, Pitman NI, McInnes IB. Disease-associated functions of IL-33: the new kid in the IL-1 family. Nat Rev Immunol 2010; 10: 103-10.
8. Pascual-Figal DA, Januzzi JL. The biology of ST2: the International ST2 Consensus Panel. Am J Cardiol 2015; 115: 3B-7B.
9. Andersson P, Yang Y, Hosaka K, et al. Molecular mechanisms of IL-33-mediated stromal interactions in cancer metastasis. JCI Insight 2018; 3.
10. Veeraveedu PT, Sanada S, Okuda K, et al. Ablation of IL-33 gene exacerbate myocardial remodeling in mice with heart failure induced by mechanical stress. Biochem Pharmacol 2017; 138: 73-80.
11. Sanada S, Hakuno D, Higgins LJ, Schreiter ER, McKenzie AN, Lee RT. IL-33 and ST2 comprise a critical biomechanically induced and cardioprotective signaling system. J Clin Invest 2007; 117: 1538-49.
12. Ghali R, Altara R, Louch WE, et al. IL-33 (Interleukin 33)/sST2 axis in hypertension and heart failure. Hypertension 2018; 72: 818-28.
13. Gu L, Li J. Short-term and long-term prognostic value of circulating soluble suppression of tumorigenicity-2 concentration in acute coronary syndrome: a meta-analysis. Biosci Rep 2019; 39: BSR20182441.
14. Michalska-Kasiczak M, Bielecka-Dabrowa A, von Haehling S, Anker SD, Rysz J, Banach M. Biomarkers, myocardial fibrosis and co-morbidities in heart failure with preserved ejection fraction: an overview. Arch Med Sci 2018; 14: 890-909.
15. Miller AM, Xu D, Asquith DL, et al. IL-33 reduces the development of atherosclerosis. J Exp Med 2008; 205: 339-46.
16. Zhuang J, Han Y, Xu D, et al. Comparison of circulating dendritic cell and monocyte subsets at different stages of atherosclerosis: insights from optical coherence tomography. BMC Cardiovasc Disord 2017; 17: 270.
17. Thygesen K, Alpert JS, Jaffe AS, et al. Fourth Universal Definition of Myocardial Infarction (2018). J Am Coll Cardiol 2018; 72: 2231-64.
18. Tearney GJ, Regar E, Akasaka T, et al. Consensus standards for acquisition, measurement, and reporting of intravascular optical coherence tomography studies: a report from the International Working Group for Intravascular Optical Coherence Tomography Standardization and Validation. J Am Coll Cardiol 2012; 59: 1058-72.
19. Oteng AB, Ruppert PMM, Boutens L, et al. Characterization of ANGPTL4 function in macrophages and adipocytes using Angptl4-knockout and Angptl4-hypomorphic mice. J Lipid Res 2019; 60: 1741-54.
20. Finn AV, Nakano M, Polavarapu R, et al. Hemoglobin directs macrophage differentiation and prevents foam cell formation in human atherosclerotic plaques. J Am Coll Cardiol 2012; 59: 166-77.
21. Luan P, Jian W, Xu X, et al. NLRC5 inhibits neointima formation following vascular injury and directly interacts with PPARgamma. Nat Commun 2019; 10: 2882.
22. Murray PJ, Allen JE, Biswas SK, et al. Macrophage activation and polarization: nomenclature and experimental guidelines. Immunity 2014; 41: 14-20.
23. Turnquist HR, Zhao Z, Rosborough BR, et al. IL-33 expands suppressive CD11b+ Gr-1(int) and regulatory T cells, including ST2L+ Foxp3+ cells, and mediates regulatory T cell-dependent promotion of cardiac allograft survival. J Immunol 2011; 187: 4598-610.
24. Valgimigli M, Campo G, Malagutti P, et al. Persistent coronary no flow after wire insertion is an early and readily available mortality risk factor despite successful mechanical intervention in acute myocardial infarction: a pooled analysis from the STRATEGY (Single High-Dose Bolus Tirofiban and Sirolimus-Eluting Stent Versus Abciximab and Bare-Metal Stent in Acute Myocardial Infarction) and MULTISTRATEGY (Multicenter Evaluation of Single High-Dose Bolus Tirofiban Versus Abciximab With Sirolimus-Eluting Stent or Bare-Metal Stent in

Acute Myocardial Infarction Study) trials. JACC Cardiovasc Interv 2011; 4: 51-62.
25. Somuncu MU, Akgun T, Cakir MO, et al. The elevated soluble ST2 predicts no-reflow phenomenon in ST-elevation myocardial infarction undergoing primary percutaneous coronary intervention. J Atheroscler Thromb 2019; 26: 970-8.
26. Tabas I, Bornfeldt KE. Macrophage phenotype and function in different stages of atherosclerosis. Circ Res 2016; 118: 653-67.
27. Rogacev KS, Cremers B, Zawada AM, et al. CD14++CD16+ monocytes independently predict cardiovascular events: a cohort study of 951 patients referred for elective coronary angiography. J Am Coll Cardiol 2012; 60: 1512-20.
28. Mancini GBJ, Hartigan PM, Shaw LJ, et al. Predicting outcome in the COURAGE trial (Clinical Outcomes Utilizing Revascularization and Aggressive Drug Evaluation): coronary anatomy versus ischemia. JACC Cardiovasc Interv 2014; 7: 195-201.
29. Ahmadi A, Leipsic J, Blankstein R, et al. Do plaques rapidly progress prior to myocardial infarction? The interplay between plaque vulnerability and progression. Circ Res 2015; 117: 99-104.
30. Yan X, Anzai A, Katsumata Y, et al. Temporal dynamics of cardiac immune cell accumulation following acute myocardial infarction. J Mol Cell Cardiol 2013; 62: 24-35.
31. Methe H, Brunner S, Wiegand D, Nabauer M, Koglin J, Edelman ER. Enhanced T-helper-1 lymphocyte activation patterns in acute coronary syndromes. J Am Coll Cardiol 2005; 45: 1939-45.
32. Hong YJ, Jeong MH, Choi YH, et al. Plaque characteristics in culprit lesions and inflammatory status in diabetic acute coronary syndrome patients. JACC Cardiovasc Imaging 2009; 2: 339-49.
33. Raffel OC, Tearney GJ, Gauthier DD, Halpern EF, Bouma BE, Jang IK. Relationship between a systemic inflammatory marker, plaque inflammation, and plaque characteristics determined by intravascular optical coherence tomography. Arterioscler Thromb Vasc Biol 2007; 27: 1820-7.
34. Nasu K, Terashima M, Habara M, et al. Impact of cholesterol metabolism on coronary plaque vulnerability of target vessels: a combined analysis of virtual histology intravascular ultrasound and optical coherence tomography. JACC Cardiovasc Interv 2013; 6: 746-55.
35. Stoger JL, Gijbels MJ, van der Velden S, et al. Distribution of macrophage polarization markers in human atherosclerosis. Atherosclerosis 2012; 225: 461-8.